Regenerative Therapy 24 (2023) 11–24

Contents lists available at ScienceDirect

Regenerative Therapy

journal homepage: http://www.elsevier.com/locate/reth

Original Article

In vitro and *in vivo* evaluation of electrospun poly (ε-caprolactone)/ collagen scaffolds and Wharton's jelly mesenchymal stromal cells (hWJ-MSCs) constructs as potential alternative for skin tissue engineering

Liliana Lizarazo-Fonseca, Luz Correa-Araujo, Leonardo Prieto-Abello, Bernardo Camacho-Rodríguez, Ingrid Silva-Cote*

Tissue Engineering Unit, Instituto Distrital de Ciencia Biotecnología e Innovación en Salud – IDCBIS, Bogotá, Colombia

ARTICLE INFO

Article history:
Received 6 January 2023
Received in revised form
8 March 2023
Accepted 20 May 2023

Keywords:
Dermal substitutes
Scaffolds
Poly(ε-caprolactone)
Collagen type I
Wharton's jelly mesenchymal stromal cells

ABSTRACT

Dermal substitutes bear a high clinical demand because of their ability to promote the healing process of cutaneous wounds by reducing the healing time the appearance and improving the functionality of the repaired tissue. Despite the increasing development of dermal substitutes, most of them are only composed of biological or biosynthetic matrices. This demonstrates the need for new developments focused on using scaffolds with cells (tissue construct) that promote the production of factors for biological signaling, wound coverage, and general support of the tissue repair process. Here, we fabricate by electrospinning two scaffolds: poly(ε-caprolactone) (PCL) as a control and poly(ε-caprolactone)/collagen type I (PCol) in a ratio lower collagen than previously reported, 19:1, respectively. Then, characterize their physicochemical and mechanical properties. As we bear in mind the creation of a biologically functional construct, we characterize and assess *in vitro* the implications of seeding human Wharton's jelly mesenchymal stromal cells (hWJ-MSCs) on both scaffolds. Finally, to determine the potential functionality of the constructs *in vivo*, their efficiency was evaluated in a porcine biomodel. Our findings demonstrated that collagen incorporation in the scaffolds produces fibers with similar diameters to those in the human native extracellular matrix, increases wettability, and enhances the presence of nitrogen on the scaffold surface, improving cell adhesion and proliferation. These synthetic scaffolds improved the secretion of factors by hWJ-MSCs involved in skin repair processes such as b-FGF and Angiopoietin I and induced its differentiation towards epithelial lineage, as shown by the increased expression of Involucrin and JUP. *In vivo* experiments confirmed that lesions treated with the PCol/hWJ-MSCs constructs might reproduce a morphological organization that seems relatively equivalent to normal skin. These results suggest that the PCol/hWJ-MSCs construct is a promising alternative for skin lesions repair in the clinic.

Abbreviations: hWJ-MSCs, Wharton's jelly mesenchymal stromal cells; PCL, Poly(ε-caprolactone); PCol, Poly(ε-caprolactone)/Collagen type I; PCol/hWJ-MSCs, Constructs of Poly(ε-caprolactone)/Collagen type I and Wharton's jelly mesenchymal stromal cells; PDGF-AA, Platelet-derived growth factor; b-FGF, Basic fibroblast growth factor; TGF-β1, Transforming growth factor beta 1; JUP, Plakoglobin; SEM, Scanning electron microscopy; XPS, X-Ray Photoelectron Spectroscopy; DSC, The Differential Scanning Calorimetry; HMDS, 1,1,3,3,3-Hexamethyldisilazane; TFE, 2,2,2-Trifluoroethanol; GFP-hWJ-MSCs, Human Wharton's jelly mesenchymal stromal cells expressing green fluorescent protein; TCP, Tissue culture plate; DMEM, Dulbecco's Modified Eagle Medium- Thermo Fisher Scientific; hPL, Human platelet lysate; hEGF, Human endothelial growth factor; KGM, Keratinocyte Growth Medium; qRT-PCR, Quantitative real-time polymerase chain reaction.

* Corresponding author. Secretaría Distrital de Salud, Carrera 32 # 12-81, Bogotá, Colombia
E-mail address: izsilva@idcbis.org.co (I. Silva-Cote).
Peer review under responsibility of the Japanese Society for Regenerative Medicine.

https://doi.org/10.1016/j.reth.2023.05.005

1. Introduction

As the human body's largest organ, the skin is susceptible to wounds from interacting with the environment. A primary mechanism to start wound healing is supported by stem cells located in the epidermis and dermis [1]. However, full-thickness wounds where skin stem cells are compromised require autografts or allografts, which would be necessary for covering the affected area and decreasing healing time [2]. When more than 50% of the total body surface area in patients with severe wounds is compromised, autograph implants are disadvantageous due to the limited availability of remnant skin without affecting the epidermal barrier and reduced immunity, the leading cause of morbidity [3]. In the case of allografts, the amount of available tissue is also a problem. This added to the use of immunosuppressants to prevent immunological graft rejection, which also increases the patient's vulnerability to viral and bacterial infections [3,4].

Current strategies for skin wound treatment are tissue-engineered skin substitutes. These synthetic and bioengineered substitutes are generally placed on the lesion to provide barrier protection against microorganisms, pain reduction, and promote wound healing through tissue regeneration [4–6]. Tissue engineering is an evolving field, developing new technologies and methodologies to generate skin substitutes that achieve complete tissue repair, preserving skin elasticity and decreasing scar formation.

Methodologies used to generate skin substitutes by tissue engineering are films, hydrogels, and polymeric scaffolds from electrospinning and 3D printing [7,8]. Scaffolds must reach the standard parameters of the native matrix, e.g., biocompatibility, biodegradability, easy handling, and low cost. Synthetic polymers such as polyesters, polytetrafluoroethylenes, and polyurethanes manufacture this scaffold type [9]. In addition, natural polymers, mainly proteins, and polysaccharides, in combination with synthetic polymers, have been used to generate structures with better mechanical properties improving cell adhesion, survival, proliferation, and differentiation [10].

Otherwise, skin substitutes, including differentiated embryonic cells, induced pluripotent stem cells, human dermal fibroblasts [11], foreskin-derived keratinocytes [12], keratinocyte stem cells [13], hair follicle stem cells [14], bone marrow-derived [15], adipose tissue-derived [16] and umbilical cord Wharton's jelly-derived mesenchymal stromal cells [17] has been used for enhancing wound healing. Special consideration offered by mesenchymal stem cells is due to their recognized ability to produce paracrine factors that may be useful in regeneration and wound healing.

In this study, we have designed a skin substitute resulting from a biosynthetic scaffold and Wharton's jelly mesenchymal stromal cells. Using the electrospinning technique first, we made a scaffold from poly(Ɛ-caprolactone) and collagen type I in a proportion 9:1. Then, hWJ-MSCs were added to explore whether this combination provides a better potential therapeutic strategy in skin tissue repair.

Biopolymeric scaffolds were characterized by analyzing the structural, morphological, mechanical, and biocompatibility properties. In addition, in the PCol/hWJ-MSCs construct, growth factor expression (PDGF-AA, b-FGF, Angiopoietin I, TGF-β1) was measured, and their inductive differentiation effect was assessed using epithelial differentiation markers (plakoglobin and involucrin) expression as reporters. Furthermore, we explored the ability of the PCol scaffold and PCol/hWJ-MSCs construct to induce skin repair after surgical implantation in porcine biomodels for 30 days; histological stains evaluated the repair process. Our results demonstrate that the PCol/hWJ-MSCs construct might be a skin repair and wound-healing alternative, brightening the landscape for skin lesions treatment in the clinic.

2. Materials and methods

2.1. Fabrication process of electrospun scaffolds

For PCol and PCL scaffolds (used as a control) fabrication, poly ε-caprolactone (MW ~ 80,000 g/mol) pellets (PCL, Sigma Aldrich CAS No. 24980-41-4) were dissolved in 2,2,2-Trifluoroethanol ≥99% (TFE, Merck) at 85.5 mg/mL, collagen type I from calf skin (Sigma-Aldrich CAS No. 9007-34-5) was added to the respective solution at 4.5 mg/mL to obtain a total polymer concentration in a 9% w/v. Solutions were maintained under magnetic stirring at 500 rpm for 6 h. Each solution was loaded into a 10 mL syringe with a blunt-tipped needle and internal diameter of 0.8 mm and incorporated into the injection system (NE injector model 4000 Syringe Pump Company) of the electrospinning equipment (High voltage power supplies Genvolt 7 × 30). For the PCol solution (9% w/v), a voltage of 19 kV was applied, a needle-to-collector distance of 15 cm, and a flow rate of 0.6 mL/h. For the scaffold control, PCL (9% w/v) was electrospun using a voltage of 19 kV, a distance from the needle to the collector of 15 cm, and the flow rate was increased to 1 mL/h due to the change in viscosity presented by the solution. The volume of the electrospun solution was 300 μL, and the obtained scaffolds were stored at 37 °C to eliminate solvent remnants.

2.2. Physicochemical scaffold characterization

2.2.1. Morphology and diameter analysis of electrospun microfibers

The morphology and diameter of PCol and PCL fibers were determined by scanning electron microscopy (SEM) (JEOL-JSM-7600F) at an accelerating voltage of 20 kV after gold coating using a sputtering machine (Quorum Q150 RES). Magnifications between 5000× and 10000× were used to determine fiber diameters using the image analysis software ImageJ.

2.2.2. Surface elemental composition

Surface chemical characterization of the scaffolds was performed by X-Ray Photoelectron Spectroscopy (XPS) at 2–3 nm deep, using a monochromatic Mg X-ray source (h = 1253.6 eV) and a photoelectron spectrometer (VG-ESCALAB) connected to an ultra-high vacuum system. Spectra were obtained with a constant energy step of 50 eV and an electron take-off angle of 45°. The deconvolution analysis of the spectra was performed with the software Origin 9®.

2.2.3. Contact angle

Determination hygroscopic properties of PCol and PCL scaffolds was performed using Pinnacle Studio software and a Ramehart Inc Model 100-07-00 goniometer. Briefly, a 2 μl drop of distilled water was deposited on the surface of the scaffolds and the angles were calculated from the contact with the scaffold and at 10 s from the drop contact in ImageJ software.

2.2.4. Thermal analysis of scaffolds

For the scaffolds' thermal transitions determination, samples were dried in a desiccator using a vacuum pump (VacuuBrand model RZ 2.5). Subsequently, 10 mg of sample were placed in the Differential Scanning Calorimetry (DSC) Q100 equipment (TA Instruments). To evaluate poly(ε-caprolactone) transitions, a material heating-cooling cycle was performed from −60 °C to 150 °C and from 150 °C to −60 °C, and for the collagen, a heating ramp from 0 °C to 300 °C with a temperature ratio of 20 °C/min under an N_2 atmosphere to find the thermal transitions.

2.3. Mechanical characterization of scaffolds

The electrospun scaffolds (n = 6) tensile strength was determined using a universal tensile testing machine (INSTRON 5500R, Instron Inc., MA, USA). The tensile test was carried out using 500 N load cell at a rate of 10 mm/min on the specimen. The scaffolds were evaluated by uniaxial tension according to ASTM D1708. Young's modulus of the specimens was estimated from the slope of the unloading curve in the region of maximum load.

2.4. Tissue constructs formation and characterization

To assess the formation of tissue constructs, we first evaluated whether the PCol and PCL scaffolds were cytocompatible and promoted cell proliferation. For this purpose, the scaffolds were cut with a 1 cm diameter punch and subsequently sterilized with gamma radiation. Then human Wharton's jelly mesenchymal stromal cells expressing green fluorescent protein (GFP- hWJ-MSCs) were seeded at a density of 5×10^4 in Dulbecco's Modified Eagle Medium (DMEM- Dulbecco's Modified Eagle Medium-Thermo Fisher Scientific) supplemented with 10% human platelet lysate (hPL) plus 1% antibiotic - antimycotic and incubated at 37 °C in a 5% CO_2 atmosphere. Cells were observed throughout the culture at 24, 48, and 120 h with a fluorescence microscope (LEICA DMi8-M), photographic record was done at each time point. Fluorescence images were analyzed in the software ImageJ. First, the color layers of the image were separated to get the green color. Then the contrast, brightness, background, and threshold were adjusted to obtain a black-and-white image with clearly separated cells, and the particle analyzer of the software was used to get the cell count. Statistical treatment of the images in triplicate was performed with the software R®, using Duncan's multiple comparison test.

Likewise, hWJ-MSCs, previously isolated and characterized [18], were seeded on the scaffolds and cultured for 1, 3, 5, and 7 days, their metabolic activity was determined using the resazurin assay (Sigma-Aldrich, St Louis, MO, USA). Briefly, 5×10^4 hWJ-MSCs (n = 3 donors) were seeded on 1 cm diameter scaffolds and placed on a 24-well plate. After each experimental time, the medium was changed to 500 μl of a 1% resazurin solution in fresh culture medium and incubated for 3 h, the supernatant (100 μL) was collected, and the 570 nm and at 600 nm absorbance was measured on a microplate reader (Synergy; BioTek, USA). Data were represented as the mean ± standard deviation. Statistical significance was tested using a student's t-test, and p-value <0.05 were considered significant.

2.4.1. Analysis of growth factors production involved in skin tissue regeneration, modulated by scaffolds

To assess whether hWJ-MSCs produced growth factors associated with wound repair in the constructs, we seeded 5×10^4 hWJ-MSCs (n = 3 donors) on 1 cm diameter scaffolds (PCol and PCL) and maintained at standard conditions. Supernatants were collected at 12, 24, 48, 72, and 96 h and centrifuged at 1200 rpm for 6 min to remove cell debris and stored at −20 °C. Protein concentration in the hPL-supplemented culture medium was also measured to estimate the levels of each growth factor before incorporation into the constructs. hWJ-MSCs seeded on the tissue culture plate (TCP) were also considered a control.

The production of four determinant growth factors in the skin lesion repair as platelet-derived growth factor (PDGF-AA), basic fibroblast growth factor (b-FGF), Angiopoietin I and transforming growth factor beta 1 (TGF-β1) was evaluated using a magnetic bead-bound immunoassay (Luminex LXSAHM-08 R&D Systems Minneapolis, USA), according to the manufacturer's instructions. Briefly, 50 μl of conditioned medium was incubated with 50 μl of magnetic microparticles for 2 h; the microparticles were washed and incubated with the biotin-antibody cocktail mixture for 1 h at room temperature. After washing, streptavidin-PE was added to the microparticles for 30 min and incubated at room temperature. The microparticles were washed and resuspended before reading on Luminex. The data were processed using GraphPad Prism 7 to observe the behavior in the production of soluble factors in each construct at different times.

2.4.2. hWJ-MSCs differentiation on the constructs

For epithelial differentiation, 2.6×10^4 hWJ-MSCs were seeded on a 1 cm diameter scaffold in keratinocyte basal medium supplemented with 0.4% bovine pituitary extract, 0.01% human endothelial growth factor (hEGF), 0.01% insulin, 0.01% hydrocortisone and 0.01% antibiotic-antimycotic, (KGM Keratinocyte Growth Medium BulletKit w/o Ca^{++}, Lonza) and in low glucose DMEM medium supplemented with 10% hPL, plus 1% antibiotic-antimycotic as a differentiation control. The culture media was changed to a fresh one every 3 days. The assessment of differentiation was carried out by observation of cell micromorphology by SEM and epithelial markers by gene expression analysis of Involucrin and JUP using quantitative real-time polymerase chain reaction (qRT-PCR) at 7 and 14 days of culture.

2.4.3. Micromorphology analysis of differentiated cells by SEM

The micromorphology of hWJ-MSCs cultured on the electrospun scaffolds cultured with DMEM medium and KGM medium was observed by SEM. Briefly, after removing the culture medium, the constructs were washed with 1X PBS twice, fixed in 4% PFA for 1 h, followed by two washes with deionized water. The constructs were then subjected to gradient dehydration with ethanol at 30%, 50%, 70%, 90%, and 96% for 15 min and 100% twice for 15 min. The scaffolds were then desiccated to the critical point with, 1,1,3,3,3-Hexamethyldisilazane (HMDS) CAS No. 999-97-3 (Sigma Aldrich) in three washes of 10 min each. Finally, the solvent was removed and dried at room temperature. Then a gold coating under vacuum was performed using a sputtering machine (Quorum Q150 RES) at 1 kV and 5 mA for 60 s. The gold coated samples were imaged by SEM (JEOL-JSM-7600F) at an accelerating voltage of 20 kV; magnifications of 500× and 5000× were used, and images were processed using the software ImageJ.

2.4.4. Relative gene expression by qRT-PCR

Total RNA from hWJ-MSCs, both differentiated or undifferentiated, seeded in PCL or PCol scaffolds, was isolated at 7 and 14 days post-cultured by a PureLink RNA Mini Kit (Thermo Fisher Scientific, Waltham, Massachusetts, USA) according to the manufacturer protocol. RNA concentration and quality were assessed on a NanoDrop-1000 instrument (Thermo Scientific NanoDrop™ 2000/2000c). Complementary DNA was prepared by reverse transcription of total RNA using SuperScript™ IV First-Strand cDNA Synthesis Reaction (Invitrogen, San Diego, CA, US), followed by qRT-PCR using a 7500 Fast Real-Time PCR System (Applied Biosystems, California, USA). These reactions used TaqMan gene expression assays (Applied Biosystems, California, USA). Each reaction contained 5 μL of Master Mix (Applied Biosystems), 2.5 μL of molecular biology grade ultrapure water, 0.5 μL Taqman Assay and 2 μL of cDNA. Epithelial differentiation genes such as Involucrin (IVL, Hs00846307_s1), Junction Plakoglobin (JUP, Hs00158408_m1), and housekeeping gene β-actin (Hs01060665_g1) were analyzed. qRT-PCR efficiency for each gene was determined based on the calibration curve using formula E = 10(−1/slope)- 1. Relative gene expression was subsequently

calculated using the 2-ΔΔCT method. The heatmap of the related data was made in the online software Displayr.

2.5. In vivo wound healing evaluation

Six 10-week-old Yorkshire pig biomodels weighing approximately 45 kg, female, were used. Animals were anesthetized with Isoflurane 3% by inhalation for 7–10 min until surgical anesthesia. The whole dorsum was then shaved and washed with Chlorhexidine® soap. With the animals in a prone position, the wound region was delimited with a sterile acetate frame, and each lesion area was 9 cm^2 (3 × 3 cm) and 5 cm between wounds. Immediately, four full-thickness wounds were surgically created on the back of each animal with a scalpel (removal of dermis, epidermis, and hypodermis). The incision was extended down to the subcutaneous cellular tissue, and each wound was covered with the respective tissue construct or scaffold, and one wound received no treatment (negative control).

The PCol/hWJ-MSCs constructs and the PCol scaffolds were implanted on a full-thickness wound in healthy female Yorkshire pig biomodels and compared to the negative control (untreated wound) to evaluate whether the construct had the potential for skin lesion repair. All animal protocols were submitted and approved by the Institutional Animal Care and Use Committee (IACUC) of ANESTCOL S.A. Bogota, Colombia (Protocol Number: 094). The hWJ-MSCs (1×10^6 cells) in passage five were seeded on a 9 cm^2 PCol scaffold and incubated at 37 °C, 19% humidity, and 5% CO_2 to obtain the constructs 24 h prior to surgery.

Constructs or scaffolds were sutured through the wound edge and the center of the lesion. Then, each wound was covered with a transparent silicone sheet and with a bandage surrounding the dorsum of each biomodel. After 30 days, euthanasia was performed to obtain tissue from the repaired area for the different evaluated conditions and additionally for healthy skin. These samples were fixed with PFA 4%. Paraffin embedding tissue was sectioned at 4 μm, and sections were stained with hematoxylin&eosin and Masson trichrome stains. The slides were observed at 10× and 20× magnification for histological evaluation.

3. Results

3.1. Scaffold morphology

According to SEM image analysis, fibers with size under a micrometer without defects and randomly oriented were observed for both PCL and PCol (Fig. 1a and b). The PCL scaffold showed fibers with an average diameter of 804 ± 186 nm (Fig. 1c), while in the PCol scaffold, the fiber diameter was 390 ± 71 nm (Fig. 1d). Importantly this noticeable reduction in the diameter may be associated with amide content in the collagen.

3.2. Scaffold surface

For the PCL spectra (Fig. 2a and b), C1s and O1s signals were detected; with regards to C1s, four signals are presented (C–C/C–H at 284.6 eV, C–O at 285.7 eV, O–C–O at 287.5 eV and O–C=O at 288.7 eV) and for O1s two signals (*O–C=O at 533.1eV and O–C=O* at 531.7eV) which matches with the XPS analysis reported in the literature for the PCL [19,20]. The XPS results of the PCol scaffold show a signal attributed to N1s, which corresponds with the presence of collagen on the scaffold surface (Fig. 2c), thus confirming the successful immobilization of the protein on the fiber surface, which has been shown to improve cell adhesion and proliferation. The atomic composition percentage (Fig. 2d) shows 41.82% of surface oxygen in the PCL scaffold and 43.82% and 2.49% of oxygen and nitrogen, respectively, for PCol scaffolds, reaffirming the presence of collagen in the PCol surface.

3.3. Contact angle

Surface wettability is an important property of biomaterials and can affect cell adhesion and proliferation. The affinity of water to the nanofibrous matrix was studied by contact angle (Fig. 3).

The PCL scaffold's contact angle was 123.31° ± 1.81° at the moment of drop contact with the scaffold, after 10 s it was 109.42° ± 5.22° (Fig. 3b), which results from crystalline regions in its structure, data similar to those found by other authors [21,22]. For the PCol scaffold, it was 75.73° ± 4.27° and 62.75° ± 1.87° at 0 and 10 s, respectively, (Fig. 3b). Considering the contact angle values obtained during the tests, the influence of collagen incorporation in the PCL scaffolds is evident, generating more hydrophilic scaffolds.

3.4. Thermal analysis

As shown in Fig. 4a, the crystallization temperature (Tc) 32.39 °C, the melting temperature (Tm) 57.42 °C and the glass transition temperature (Tg) −59.53 °C of PCL are similar to values reported on the literature [23]. A heating ramp from 0 °C to 300 °C was used to identify the different collagen denaturation temperatures and to get the DSC thermogram shown in Fig. 4b. Given the fact that collagen can dehydrate or denature when heated, characteristic endothermic peaks in the DSC thermogram are evident at 79.50 °C attributed to the removal of free water, with a high enthalpy value of 119.7 J/g and a second signal at 186.51 °C with an enthalpy of 85.14 J/g. These signals have often been referred to as collagen dehydration temperature (TD) [24].

In Fig. 4c it is seen that the PCol scaffold temperatures 31,04 °C and 56,77 °C, Tc and Tm respectively, got decreased in comparison to PCL, this is attributed to the presence of collagen in the scaffold. The crystallinity percentage (Xc) of the PCL and PCol scaffolds was also calculated using the following equation:

$$x_c(\%) = \left(\frac{\Delta H_{m\ sample}\left(\frac{J}{g}\right)}{\Delta H_m^o\left(\frac{J}{g}\right)} \right) \times 100$$

Eq. (1). Crystallinity percentage by difference of melting enthalpies.

Where $\Delta H_m^o = 139.5$ J/g is the fusion enthalpy of 100% crystalline synthetic polymer. The PCL scaffold crystallinity percentage corresponded to 42.50%, and for the PCol scaffold, 41.53%.

3.5. Mechanical properties by uniaxial tension testing

Electrospinning is a technique used to obtain microporous fibrous structures, which significantly decreases the mechanical properties of the materials. For example, an 80 KDa PCL scaffold obtained by extrusion can exhibit Young's modulus of 190 ± 60 MPa [25] compared to 22.63 ± 2.48 MPa found in the PCL electrospun membrane. Likewise, in the PCol scaffold, Young's modulus was decreased to 6.98 ± 2.39 MPa due to the presence of collagen, matching with previous studies [26,27]. These results are attributed to the possible electrostatic interactions generated between the collagen and the PCL chains that decrease the resistance to deformation, resulting in more fragile fibers. For this reason, Young's modulus of PCol is lower than reported for skin obtained from the abdomen and back, which are 14 MPa [28] and 14,96 MPa [29].

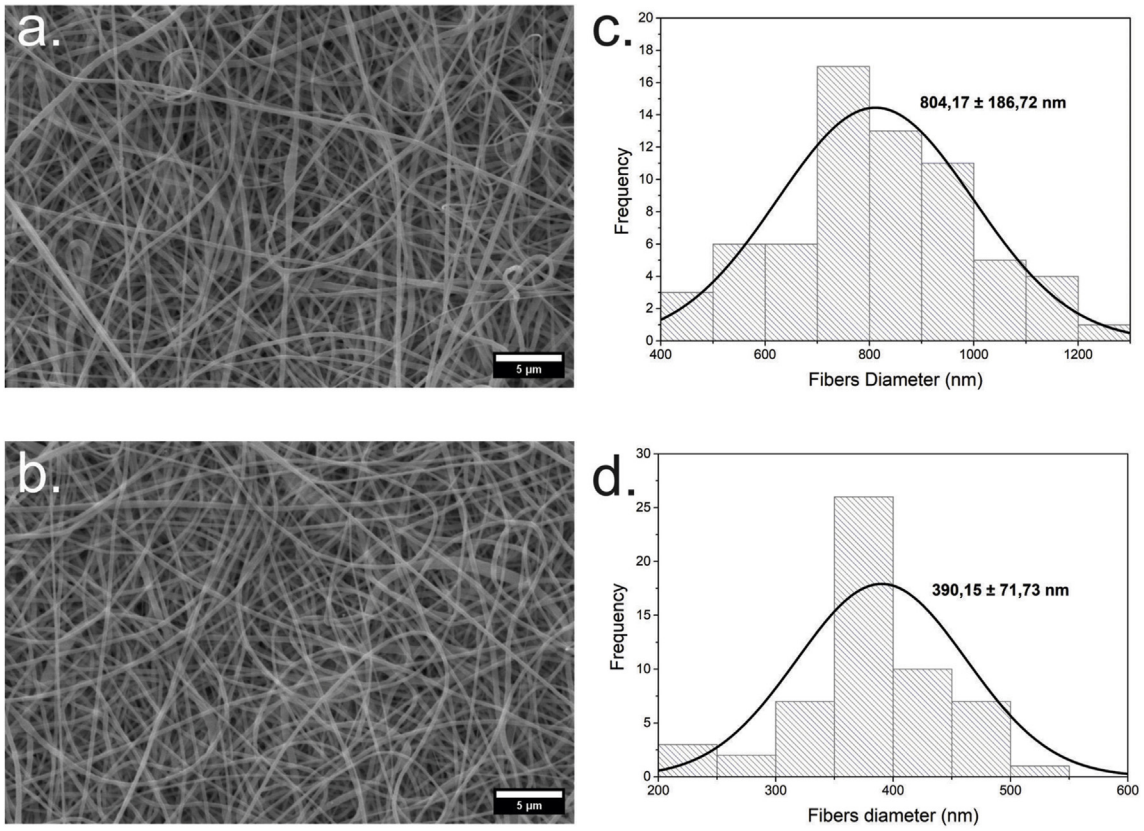

Fig. 1. SEM images of the scaffold at a magnification of ×1000 (scale bar 5 µm) and diameter distribution of random fibers of (a) PCL and (b) PCol.

On the other hand, the stress-strain graph of the PCL and PCol scaffolds can be observed in Fig. 4d, where the elastic behavior of the materials increases gradually, without bottleneck formation, because there is no reduction of the cross-sectional area before rupture. The strain percentages exceed 100%, coinciding with values previously reported by other authors [30]. These elongation values are attributed to the collagen elasticity conferred to the fibers and a possible fibers rearrangement due to the tension exerted, allowing the material to elongate without generating breakage.

3.6. In vitro interactions between cells and scaffolds

Determination of *in vitro* cells viability on the scaffolds is essential to determine if they are suitable to form tissue constructs; this is done in order to verify that the scaffold provides a proper environment to maintain viable cells and allow their proliferation. Therefore, monitoring of GFP-hWJ-MSC culture on PCol and PCL scaffolds was performed *in vitro* through fluorescence microscopy images at three time points (24, 48, and 120 h), as shown in Fig. 5. On the collagen scaffold, hWJ-MSCs have typical fibroblast-like morphology at 24 h (Fig. 5a), compared to the spheroid morphology found in the PCL scaffold (Fig. 5d). Thus, indicating that the low cell adhesion to the scaffold could be attributed to the material hydrophobicity.

However, an improvement in the morphological characteristics of the cells is observed in the PCL scaffold, as indicated by the change from the spheroid cells at 24 h (Fig. 5d) to spindle-shaped, fibroblast-like at 48 h Fig. 5e). Thus, after a surface adaptation period, cells could spread and proliferate after five days of culture (Fig. 5f). However, the increase in cell density on PCol was significantly higher (Fig. 5b, c, and g). These results were correlated with the metabolic activity data for cell proliferation. Fig. 5h shows the increase in resazurin reduction over time for PCL and PCol scaffolds. The presence of collagen significantly increases cell proliferation, indicating that the change in scaffold surface hydrophobicity favors hWJ-MSCs cell proliferation over time. According to all, we established that PCol is a biocompatible scaffold that allows cell proliferation. Then, we elaborated strategies to assess the construct's functionality *in vitro* and *in vivo.*

3.7. Growth factors involved in skin tissue regeneration

In the skin repair process, growth factors are multi-functional signaling molecules that coordinate the process of wound healing. We evaluated whether some of the main growth factors involved in skin repair (PDGF-AA, b-FGF, Angiopoietin I, and TGF-β1) were produced by hWJ-MSCs on the scaffolds. With that purpose in mind, cells were seeded on the scaffolds, and supernatants were collected at 12, 24, 48, 72, and 96 culture hours to evaluate growth factor production by an immunoassay methodology based on magnetic microspheres (Luminex). In addition, culture media (Fig. 6, dotted line) and hWJ-MSCs under standard culture conditions (Fig. 6, TCP) growth factor concentration were also evaluated.

The results show a 620.68 pg/mL PDGF-AA concentration in the culture medium and a tendency to its consumption over time (Fig. 6a). PDGF-AA is a mitogenic factor involved in cell division and proliferation, which promoted its consumption by cells [29]. The PCol construct revealed a higher factor consumption than the construct with PCL, which can correlate with the PCol higher cell proliferation rate.

In contrast, as shown in Fig. 6b, b-FGF concentration in the culture media is low (dotted line), 11.08 pg/mL, while in the

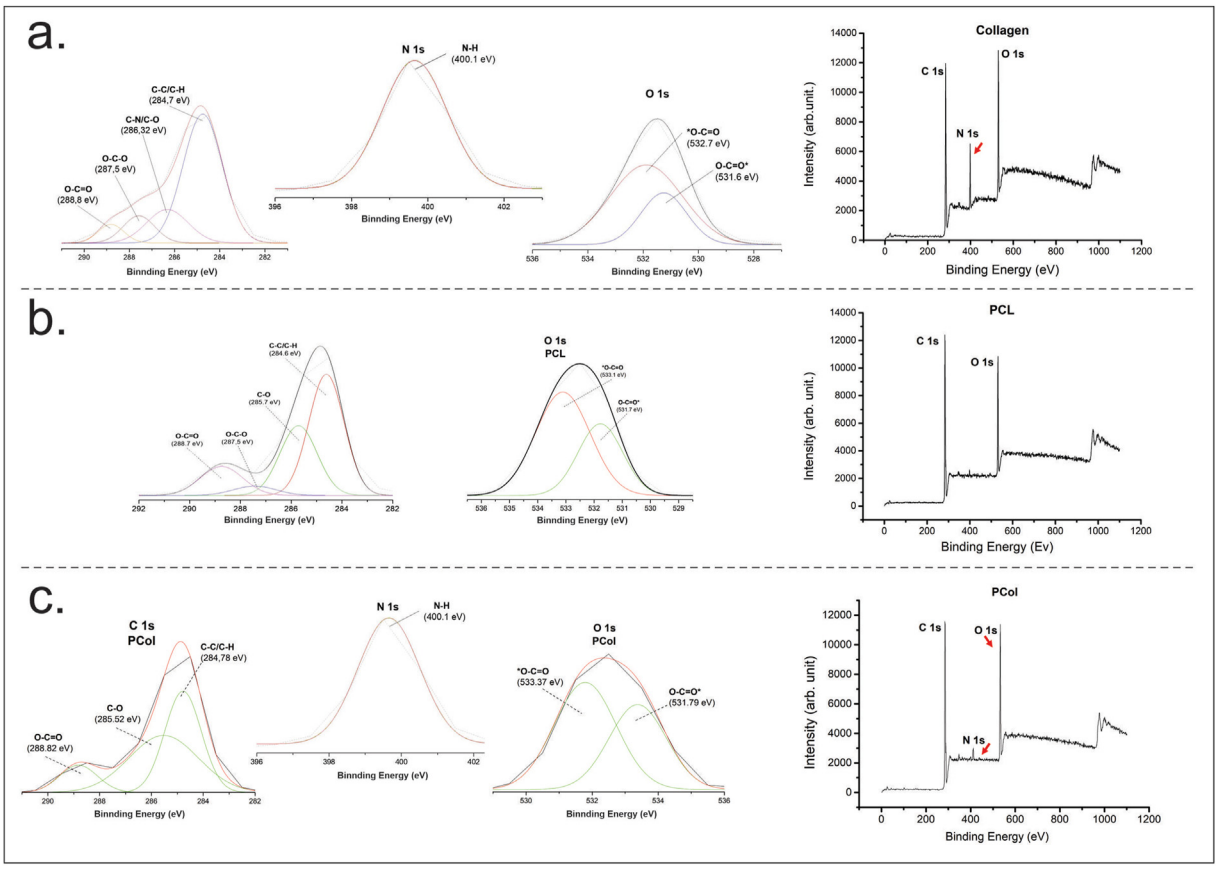

d.

COMPOSITION [AT. %]

	C1s	O1s	N1s
PCL	58,18	41,82	-
COLLAGEN	44,48	38,54	16,97
PCol	53,69	43,82	2,49

Fig. 2. General XPS survey scan of (a) Collagen, (b) PCL, and (c) PCol; Left side inserted spectra XPS C1s, O1s, and N1s peak decomposition. The red arrows indicate the characteristic peaks for the O and N signals, which for PCol are both identified, demonstrating that collagen is located on the surface of the electrospun fibers. (d) Quantification of atomic composition from XPS spectra.

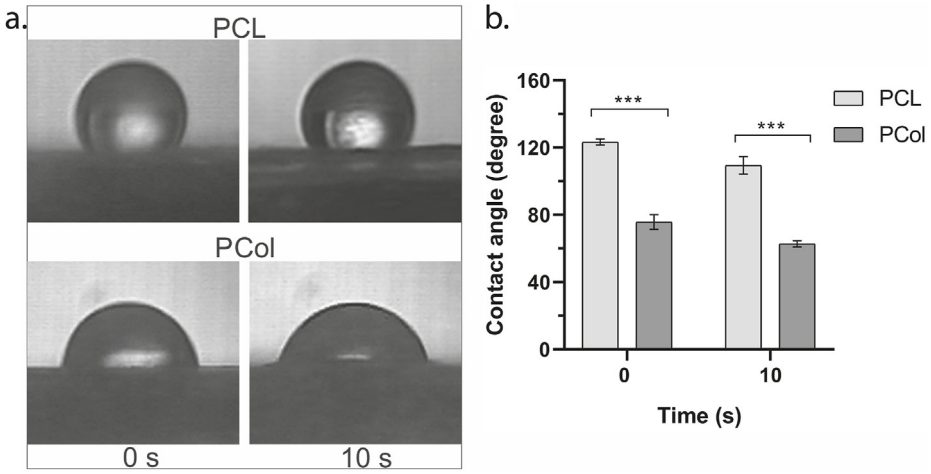

Fig. 3. (a) Droplets images on the scaffolds at the beginning of contact and after 10 s. (b) Contact angle measurement for PCL and PCol scaffolds using a two-way ANOVA, and p-value <0.05.

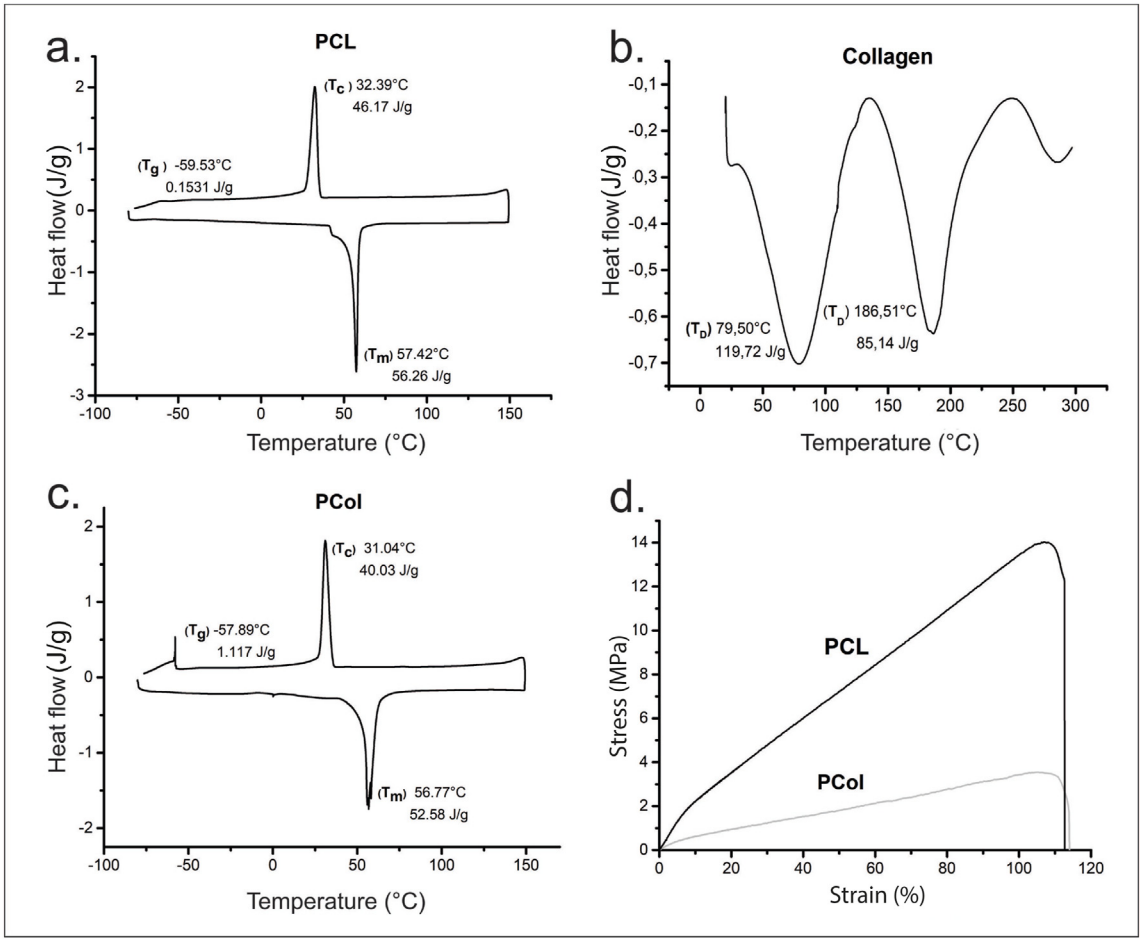

Fig. 4. Thermal properties of polymers (a) PCL, (b) collagen, and (c) PCol scaffolds were evaluated by differential scanning calorimetry (DSC). (d) Stress-strain diagram and compressive modulus for PCol and PCL scaffolds.

constructs, there is an increase in its secretion when compared to the control group (TCP) up to 72 h. These results suggest that the scaffold may induce factor secretion in the first three days of culture, evidencing the microenvironment effect on growth factors secreted by cells. b-FGF is crucial in skin repair because it participates in angiogenesis, granulation tissue formation, and wound healing [31].

On the other hand, despite the high concentration of both Angiopoietin I and TGF-β1 in culture media, 7200 pg/mL and 9200 pg/mL, respectively (Fig. 6c and d), a tendency to the production of these factors is observed in the constructs elaborated with PCol and in control (TCP) after 48 h culture. However, in constructs elaborated with PCL, there is no production of Angiopoietin I but of TGF-β1. The production of these factors in the PCol construct is essential because they stimulate granulation tissue formation and modulate angiogenesis during wound healing. Overall, these results suggest that the construct may be a good candidate for use in wound repair.

3.8. Morphological changes associated with epithelial differentiation and gene expression

To evaluate scaffold-induced differentiation of hWJ-MSCs towards the epithelial lineage, cells were cultured on PCol and PCL in DMEM and KGM medium after 7 and 14 days; SEM and epithelial marker expression were assessed the cell population. SEM image analysis showed that most hWJ-MSCs cultured in PCol and PCL in DMEN medium maintained their standard spindle shape at seven days (Fig. 7a and b). Whereas, those in the KGM medium showed homogeneous, highly elongated cell morphologies with increased size and aligned on the scaffold fibers (Fig. 7c and d). Although the cells did not acquire a polygonal morphology characteristic of keratinocytes [32], we assessed whether the phenotypic changes were due to an apparent differentiation towards an epithelial lineage by the gene expression profile of the epidermal differentiation markers Involucrin and Plakoglobin (JUP) by qRT-PCR (Fig. 8).

Gene expression profile is one of the most relevant features for determining the effect of polymeric matrices on cell differentiation ability [33]. Here we report high levels of Involucrin expression in hWJ-MSCs of the construct and maintained with KGM culture medium at 14 days. In this case, gene expression increased 12-fold; likewise, we detected a marked expression of the same gene in cells cultured in PCL scaffolds and KGM medium at 7 and 14 days. These values were higher than those found in cells cultured in a tissue culture plate (TCP) with KGM, indicating an effect of PCL and PCol scaffolds on the hWJ-MSCs differentiation toward keratinocytes.

Moreover, we identified a 3-fold increase in JUP expression in hWJ-MSCs seeded on PCL scaffolds with DMEM and KGM medium at 7 and 14 days, respectively. These values were similar to those reported in cells grown on PCol with KGM medium. This result

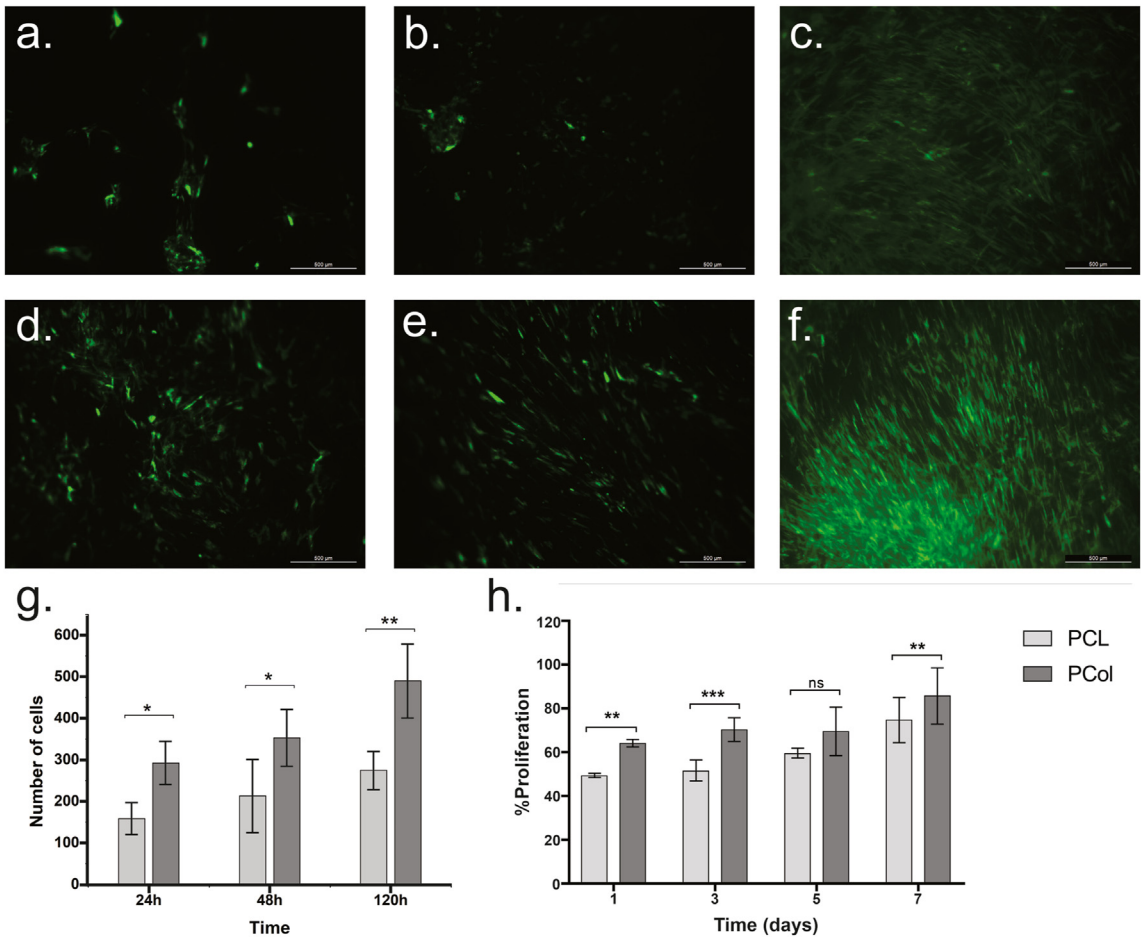

Fig. 5. *In vitro* cell morphology analysis of GFP-hWJ-MSCs seeded in electrospinning scaffolds PCol and PCL. Morphological changes were observed using a fluorescent microscope at (a) 24 h, (b) 48 h, (c) 120 h by PCol and (d) 24 h, (e) 48 h, (f) 120 h by PCL. Scale bar 500 μm. (g) Cell counting of PCol and PCL scaffold images with GFP-hWJ-MSCs. (d) Cell proliferation using the resazurin assay after 1, 3, 5, and 7 days of direct seeding of hWJ-MSCs on PCL and PCol scaffolds using a student's t-test, and p-value <0.05.

demonstrates the potential of both PCL and PCol polymeric scaffolds to induce the differentiation of hWJ-MSCs into epidermal cells due to JUP represents an essential factor in the function of epithelial cells during intercellular junction processes.

3.9. *In vivo* biocompatibility and functionality testing

In vitro biocompatibility and functionality assays suggested that the PCol and construct were suitable for further *in vivo* testing due to their ability to support cell proliferation, growth factor production, and potential to trigger differentiation of hWJ-MSCs. This experiment compared the construct with control wounds treated with the silicone sheet. The construct and the PCol scaffold showed good adherence to the wound site, and thirty days after wound creation, closure was observed to be greater than 90% in both treatments.

Wound healing was evaluated by histological analysis. The construct, formation of the basal membrane, presence of dermal papillae, and blood vessels with mild inflammatory infiltrate were evaluated (Fig. 9). Likewise, the epidermis showed its four layers (stratum corneum, lucidum, granulosa, and spinous) with moderate development of the stratum corneum (Fig. 9c and d), similar to that observed in normal skin (Fig. 9g and h). Thin parallel collagen fibers and low hyperkeratinization were also observed (Fig. 9d). On the other hand, in wounds treated with PCol scaffold, few dermal papillae and blood vessels are observed, besides a moderate inflammatory infiltrate. In the stratification of the epidermis, only the stratum corneum and lucidum are present with partial basal membrane formation (Fig. 9a). In addition, the collagen fibers are thick and without orientation (Fig. 9b). However, comparing the construct and PCol with the negative control results, it is shown that both promote wound repair more than the negative control. For this condition, inflammatory infiltrate is severe, only the stratum spinosum is observed in the epidermis (Fig. 9e), and both thick and thin collagen fibers are disorganized with hyperkeratinization (Fig. 9f).

In this sense, in the repaired skin of all the treatments, no skin appendages such as hair follicles and sebaceous glands were found. It should also be noted that, throughout the study, there were no signs of adverse effects in the local tissues (edema and erythema), maceration, or the skin surrounding the wounds in any treatments.

This trial proved that PCol membranes are flexible, easy to implant, and suture resistant. In addition, it was demonstrated that the hydrophilic membrane allows adequate contact with the wound, improving protection and cell migration functions. The collagen in the membrane guarantees the presence of amino acids or protein segments necessary for skin repair.

4. Discussion

Numerous studies have been conducted to develop new skin substitutes and improve skin repair [21,34,35]. Wound dressings

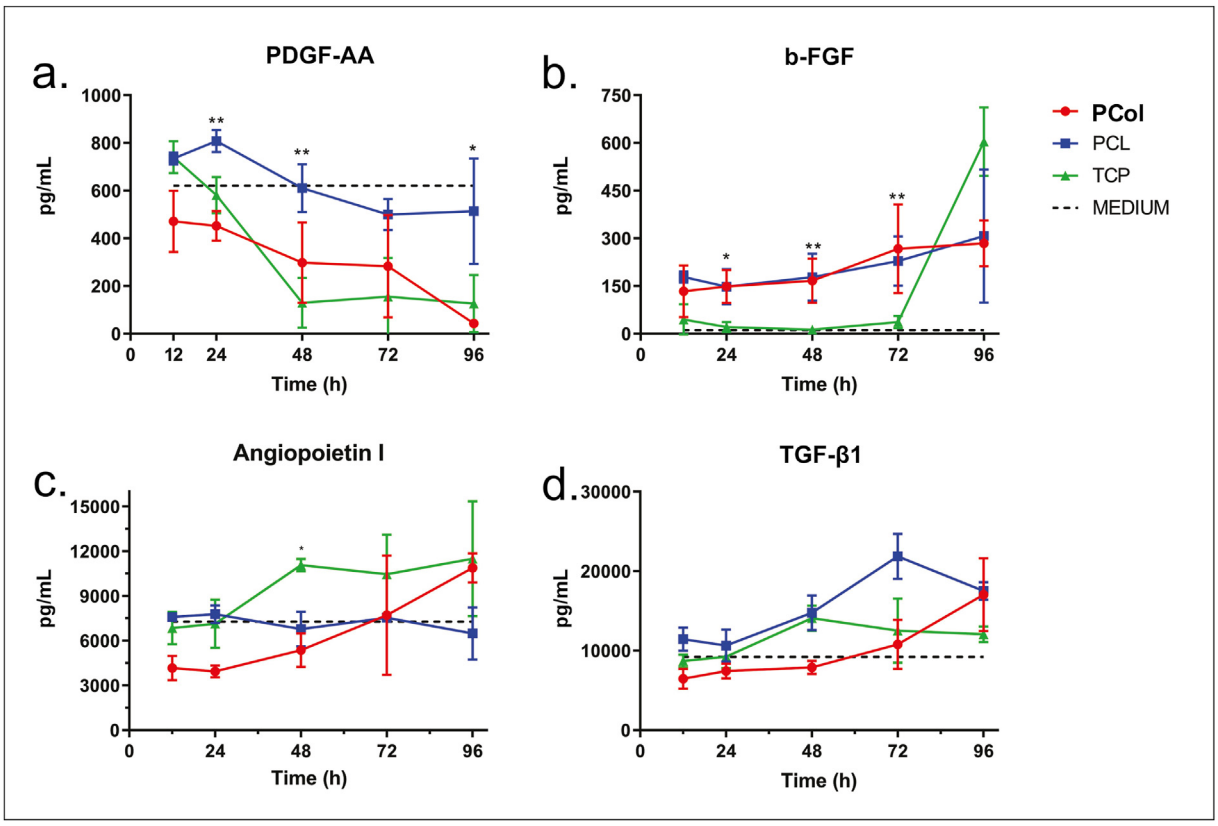

Fig. 6. Growth factors measured in supernatants from hWJ-MSCs cultured in PCol, PCL, and TCP at 12, 24, 48, 72, and 96 h (n = 3 donors) using a two-way ANOVA, and p-value <0.05.

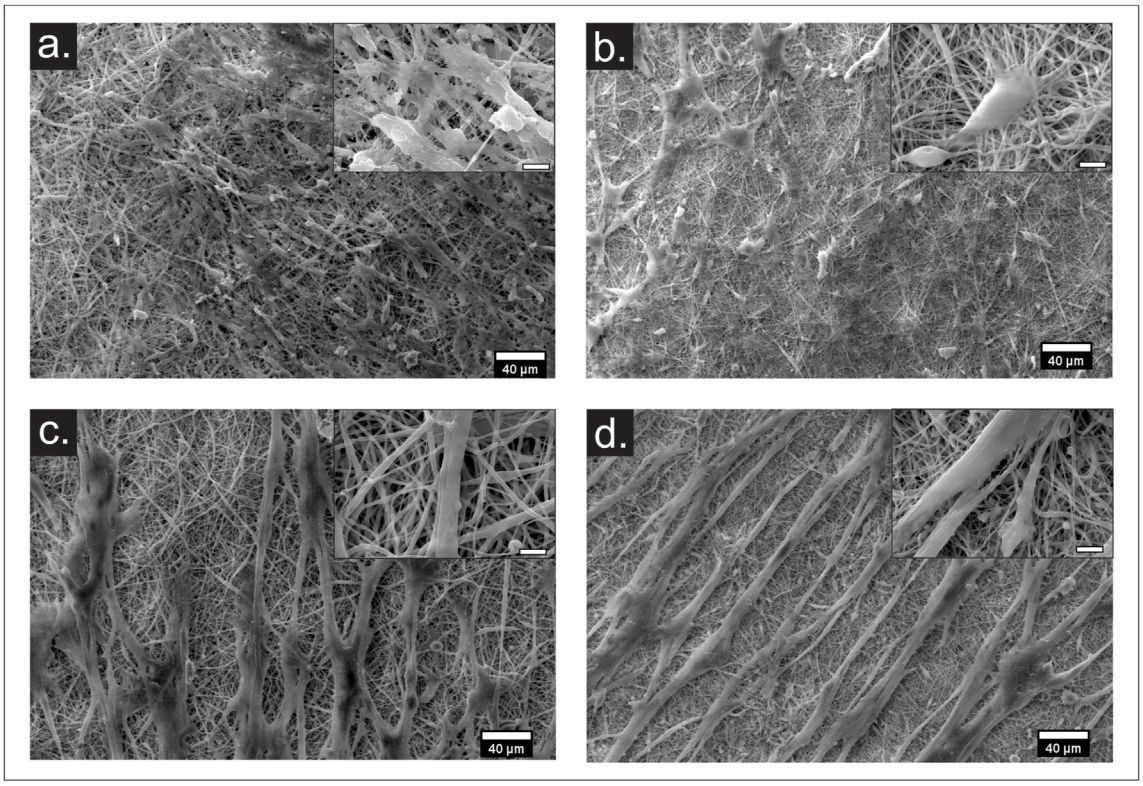

Fig. 7. SEM micrographs of Wharton jelly mesenchymal stem cells seeded on electrospun nanofibers scaffolds after 7 days in DMEM medium (a) PCL, (b) PCol, and in KGM medium (c) PCL, (d) PCol at 500× (scale bar 40 μm) and 5000× (scale bar 5 μm).

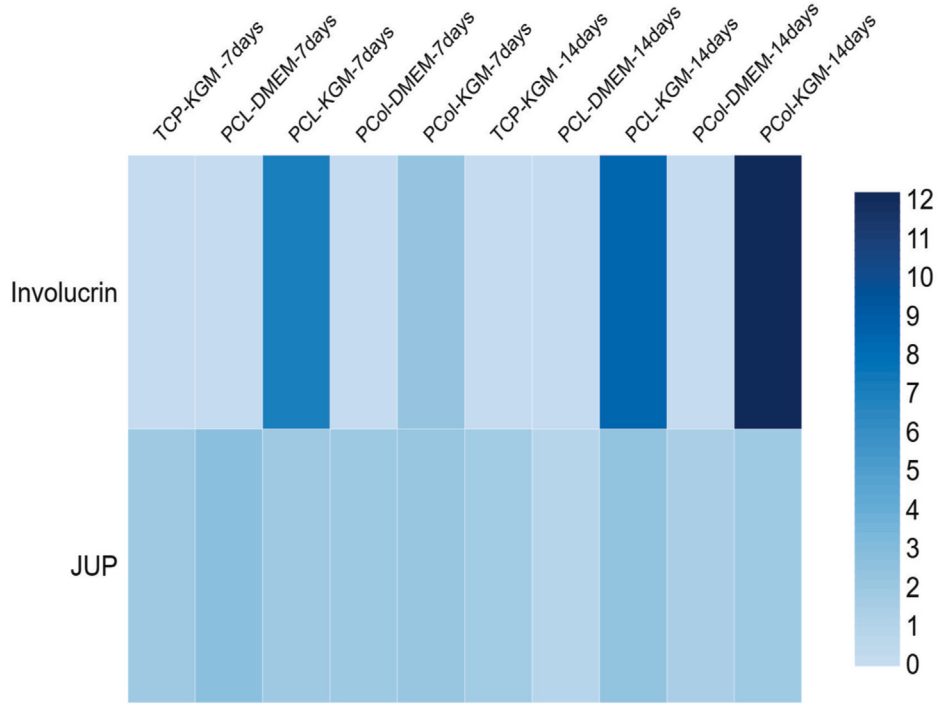

Fig. 8. The MSC-GW epithelial differentiation heat map confirmed electrospun scaffolds' supportive role for successful differentiation (n = 3) with high expression of Involucrin and plakoglobin using the 2-ΔΔCT method.

are designed to cover and protect the wound from external aggression and environmental bacteria to provide an optimal environment for healing by providing dermal factors that activate and stimulate tissue repair. In addition, recently developed products are biologically active, providing wound coverage and continuity; they also modulate wound healing by releasing growth factors and extracellular matrix components to improve the quality of healing chronic and acute wounds. These products are much more complex in structure than transitional skin substitutes and are used early to improve tissue repair or to eliminate scarring [36,37].

In this study, we fabricated a biologically active skin substitute from a PCol scaffold and hWJ-MSCs. We showed that this combination provides a better therapeutic strategy for skin tissue repair. We developed the scaffold by the electrospinning method using PCL and collagen in low proportions. PCL is a polymer with good biocompatibility, high strength, solubility, and excellent blend compatibility with natural and synthetic polymers, which is essential for the fabrication of electrospun scaffolds [38,39]. In addition, characteristics of other polymers, such as the toxic or acidic by-products of polyglycolic acid (PGA) [40] or the ability to shrink in the presence of cell culture medium of polylactic-co-glycolic acid (PLGA) [41], make PCL an adequate material to achieve the necessary mechanical and physicochemical properties for its use as a scaffold in a dermal substitute.

Likewise, we used type I collagen to manufacture the PCol scaffold because it is the most abundant protein in the human body and possesses low immunogenicity, excellent biocompatibility, and cytocompatibility. It is one of the most critical natural biomaterials used to fabricate scaffolds for tissue engineering; moreover, it plays an essential role in skin regeneration [42]. When collagen is added to the polycaprolactone polymeric matrix to fabricate the scaffolds, it provides carboxyl and amino groups that increase the conductivity of the solution, thereby reducing the force required to elongate or stretch the polymeric solution, resulting in a decrease in fiber diameter [10,43,44] as evidenced by the reduction in 51,48% of the fiber diameter of PCol compared to PCL scaffolds, this reduction is more significant than that reported by Chakrapani et al., in 2012 [45] where the fiber diameter reduction was 28% using a PCL: Collagen ratio of 3:1 in the structure a significantly higher amount of collagen than that used in our PCol scaffold (19:1).

Other changes that are observed on the PCol scaffolds are their differences in transition phase temperatures and crystallinity, where the crystalline phase in PCol scaffolds is attributed to the synthetic polymer present in the structure, which is influenced by the presence of collagen, which is introduced into the ordered region of PCL and does not allow its complete crystallization. As shown by D. Kołbuk et al., in 2013 [46]. When PCL is mixed with natural polymers such as collagen or gelatin, it becomes amorphous, which improves cell adhesion, proliferation and migration.

Similarly, the addition of collagen affects the elastic behavior of PCol, resulting in lower Young's modulus values. However, both our scaffolds (PCL and PCol) have Young's moduli greater than 3 MPa, which has been reported to be sufficient for materials used in skin tissue repair [47]. Furthermore, the deformation percentages are more significant than 100%, consistent with values previously reported by other authors [30]. This is due to collagen, which makes the scaffolds more effective in absorbing energy against an applied load through a higher degree of strain [48]. Reference values for skin tensile strength range from 4.02 to 14.93 MPa for abdominal [49] and back skin [50], respectively, and our values are within this range.

In addition, the presence of collagen functional groups in PCol significantly reduces the hydrophobicity of the scaffold, making it highly wettable. Pérez-Puyana et al., in 2021 found that the contact angle between 40 and 70° is the most indicated for cell adhesion, also that collagen concentrations affect the contact angle and are directly related to the distribution of collagen in the scaffold [51]. Where we found that a small amount of collagen is homogeneously distributed in the scaffold fibers and allows the organization of the

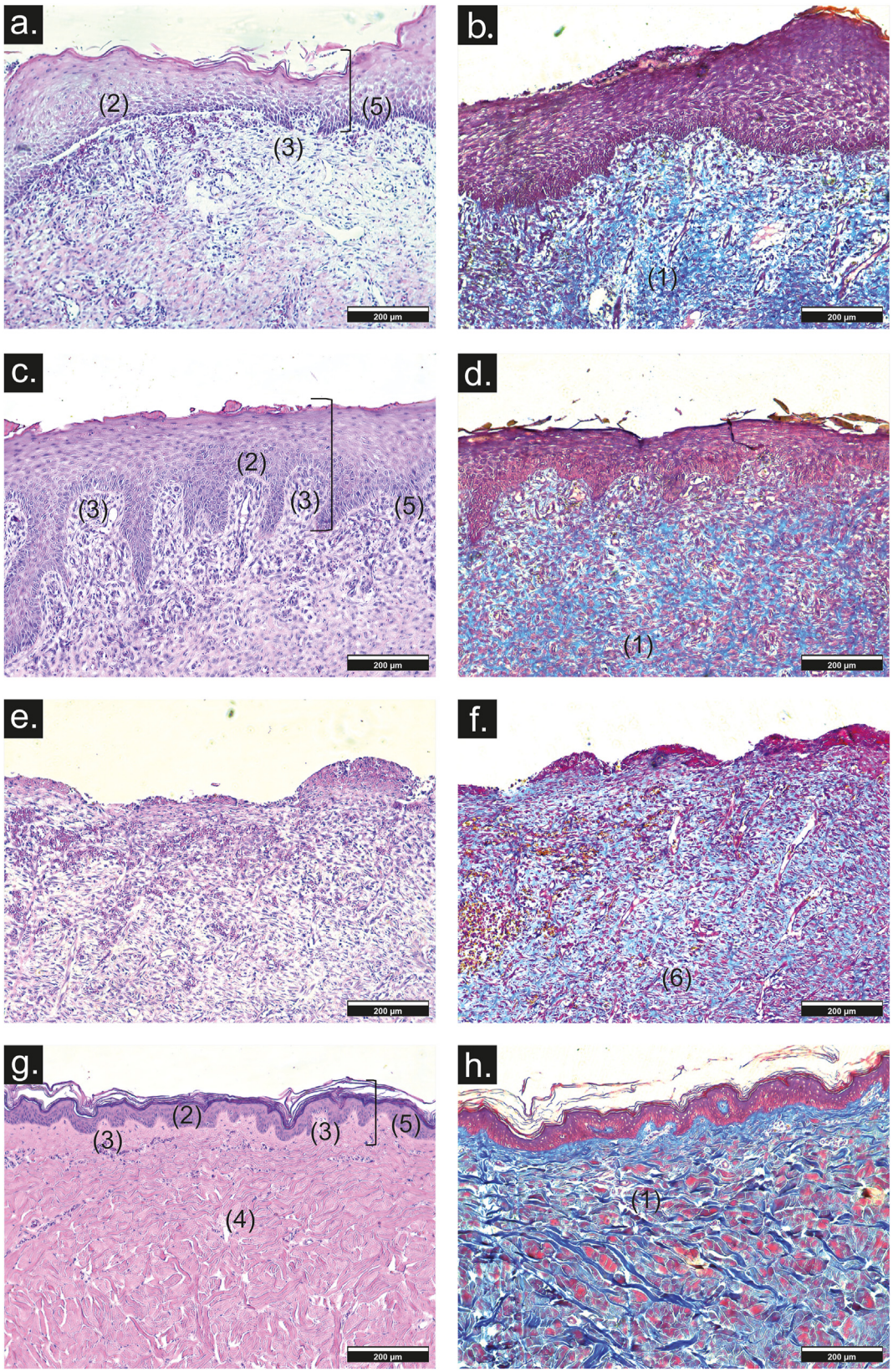

Fig. 9. Representative images of histology sections of repaired wounds at day 30 from (a, b) PCol scaffolds, (c, d) construct, (e, f) negative control, and (g, h) healthy skin (10× scale bar 200 µm). (1) collagen fiber, (2) basement membrane, (3) dermal papillae, (4) blood vessels, (5) stratification, (6) hyperkeratinization by Hematoxylin & eosin (a, c, e, g) and Masson trichrome stain (b, d, f, h).

polar groups of the proteins on the surface of the scaffold giving rise to a hydrophilic structure leading to a contact angle of 62.75° ± 1.87°, a considerable decrease in comparison to 109.43° ± 5.22°, the contact angle of PCL scaffold. Cell-scaffold interactions can be enhanced by improving surface wettability and creating a higher porosity for nutrient and waste exchange. Functional groups interacting with cadherins, integrins, and adhesion molecules in the cells are also critical. For example, biologically inert PCL nanofibers require effective surface coatings that provide adhesion molecules, such as amino groups, to promote cellular response, as shown by Zhang et al., in 2005 [52].

It is well known that hWJ-MSCs represent an attractive tool to improve engineered skin constructs as a therapeutic strategy for cutaneous lesions due to their cell plasticity, immunomodulatory capacity, and production of paracrine factors (growth factors and cytokines), which play essential roles as antioxidants, anti-inflammatories, and improve the rate of tissue repair [53]. The ability of hWJ-MSCs to differentiate into the epithelial lineage after culture under epithelial induction conditions has been previously reported [54]. However, little is known about the effect on epithelial cell differentiation when combining MSCs with biosynthetic scaffolds. Here, we investigated the ability of hWJ-MSCs to repopulate and differentiate into epithelial-like cells after culture on PCL and PCol scaffolds. Although the cells did not show morphological changes similar to keratinocytes, the gene expression profile reported high levels of Involucrin (12-fold) in the PCol/hWJ-MSCs construct in the differentiation medium. Involucrin is the terminal marker of epidermal differentiation in the upper spinous and granular layers of human skin [55], its upregulation indicates the potential of hWJ-MSCs to differentiate into epithelial cells in the construct. Furthermore, our result was similar to that reported by Ranjbarvan et al., in 2021 [56], who reported an increase in gene expression of this protein at day 10 in a co-culture of human adipose-derived mesenchymal stem cells and neonatal keratinocytes on the 3D nanofibrous PCL-platelet gel scaffold. Similarly, increased JUP expression indicates an essential signal for differentiating hWJ-MSCs into epidermal cells [54], this protein is present in both adherens junctions and desmosomes, and presumably acts as a mediator of their interactions, promoting the integrity of the epidermis [57]. The expression of these specific marker proteins confirms the transdifferentiation of hWJ-MSCs towards epithelial lineages.

We have also shown *in vitro* that the PCol/hWJ-MSCs construct produces growth factors related to tissue repair. Growth factors are signaling molecules used in various tissue engineering applications. Among them, b-FGF was the growth factor that induced secretion in the PCol/hWJ-MSCs construct from the first hours of culture and was maintained over time. It has been used for various purposes, such as *in vivo* nerve regeneration, wound healing, and induction of angiogenesis [58]. We also observed increased secretion of TGF-β in the construct after 48 days of culture. This finding is important because the secretion of collagen and other cellular matrix components is mediated by TGF-β, which is also necessary to maintain the proliferation and differentiation of cells in the wound environment [59] and has an anti-inflammatory effect [60], one of the potential factors responsible for improving healing. In addition, Angiopoietin I has been shown to promote vascular survival, inhibit vascular leakage, suppress vascular inflammation, and is essential for the proliferation of endothelial cells, fibroblasts, and keratinocytes [61,62]. In our construct, Angiopoietin I secretion was higher at 11,000 pg/mL after 96 h of culture. In contrast, the PDGF-AA levels showed an important reduction over time, indicating that consumption by cells to increase their proliferation. Altogether, the PCL and PCol scaffolds promoted the release of growth factors related to skin repair in an *in vitro* condition.

The *in vivo* evaluation of the PCol/hWJ-MSCs construct showed its capability to promote efficient repair of full-thickness skin wounds. This result suggests that in PCol/hWJ-MSCs implantation surgery, the benefit of hWJ-MSCs presence would be related to their direct scaffold colonization, regenerative ability, and paracrine effect. It is worth highlighting that no skin appendages, such as hair follicles and sebaceous glands, were found in the repaired skin of all the treatments. It should also be noted that, throughout the study, there were no signs of adverse effects in the local tissues (edema and erythema), maceration, or the skin surrounding the wounds in any treatments. In addition, the preclinical test allowed us to prove that PCol membranes are flexible, easy to implant, and suture resistant. According to histological results, no residual PCL was observed in the repaired tissues. This result is similar to those reported by Wang et al., 2016 [63] who demonstrated that tPCL (PCL and poly(ethylene oxide)) and rPCL (PCL only) grafts with a wall thickness of 777.98 ± 45.26 μm and 851.38 ± 31.81 μm, respectively, exhibited a reduction of the molecular weight of 57.3 ± 5.0% and 68.6 ± 1.7% of its initial value, after 3 months of implantation in rabbit carotid artery. In our study, the PCol scaffold thickness (38 ± 4 μm), the use of hWJ-MSCs, scaffold invasion by other cells, and enzyme production during skin repair could have accelerated scaffold degradation.

According to these results, we demonstrated that the PCol/hWJ-MSCs construct had enhance adhesion to wound, improving protection and cell migration functions. The collagen in the membrane guarantees the presence of amino acids or protein segments necessary for skin repair. Moreover, it was determined that low ratios of natural polymer to synthetic polymer could achieve similar results compared to previous research that used a high proportion of natural polymer, which improves parameters such as hydrophilicity, cell adhesion, and mechanical and surface properties [64]. Also, it is important to note that the amount of collagen, combined with the scaffold fabrication technique, allows us to use less of this protein, thus reducing the production cost of the scaffolds and enabling scale-up technology. Compared to other incorporation techniques or surface modifications, which generate additional steps in scaffold preparation and increase production costs by requiring large amounts of collagen, reagents, and costly techniques [34,65], In addition, these reagents can be toxic to cells and affect cell survival in the construct [42].

Currently, commercially available skin substitutes such as Dermagraft®, TransCyte®, Apligraft®, OrCel®, Stratagraft®, or Laserskin® are composed mainly by keratinocytes, fibroblasts, or both seeded onto PGA mesh, nylon, silicone, bovine collagen, or hyaluronic acid [66–68]. The arrangement of the scaffold and cells is similar to our construct. However, the main difference is the use of hWJ-MSCs (adult stem cells) instead of differentiated cells. These cells are immunomodulatory [69], secrete paracrine factors, and can transdifferentiate into keratinocyte-like cells.

On the other hand, this study showed the usefulness of PCol/hWJ-MSCs as a skin substitute in porcine experiments. The PCol/hWJ-MSCs construct promoted wound closure and epithelialization. We expect PCol/hWJ-MSCs to be a new and effective treatment option for acute wounds, such as burns, and chronic wounds, such as venous leg ulcers or diabetic foot ulcers. However, the next step is to establish the safety and efficacy of the PCol/hWJ-MSCs construct, which will need to be studied in clinical trials.

5. Conclusion

We obtained a PCol scaffold with mechanical properties similar to normal skin. The scaffold promotes cell adhesion, viability, and differentiation, especially towards epithelial lineage. In addition, the scaffolds of PCol stimulate the secretion of angiogenic and

epithelial growth factors involved in wound healing, which was demonstrated by the significant healing skin wounds in the porcine biomodel. These results suggest that the construct based on PCol/hWJ-MSCs is a promising alternative for skin lesions repair.

Declaration of competing interest

The authors declare that they have no conflicts of interest.

Acknowledgment

This work was supported by Instituto Distrital de Ciencia Biotecnología e Innovación en Salud through agreement 101 of 2018 “Implementación de un Banco Público de Sangre de Cordón Umbilical y una Unidad de Terapia Celular en el Hemocentro Distrital” from the Secretary of Health, Bogotá, and the Ministry of Science, Technology and Innovation (MinCiencias), from Colombia, through the Project number 739 of 2019. We also want to thank Lorena Gonzalez MSc and Carlos Ayala PhD for comments that greatly improved the manuscript.

References

[1] Frykberg RG, Banks J. Challenges in the treatment of chronic wounds. Adv Wound Care 2015;4(9):560–82. https://doi.org/10.1089/wound.2015.0635.
[2] O'Brien FJ. Biomaterials & scaffolds for tissue engineering. Mater Today 2011;14(3):88–95. https://doi.org/10.1016/S1369-7021(11)70058-X.
[3] Su JW, Mason DP, Murthy SC, Rice TW. Closure of a large tracheoesophageal fistula using AlloDerm. J Thorac Cardiovasc Surg Mar. 2008;135(3):706–7. https://doi.org/10.1016/j.jtcvs.2007.11.014.
[4] Atiyeh BS, Costagliola M. Cultured epithelial autograft (CEA) in burn treatment: three decades later. Burns Jun. 2007;33(4):405–13. https://doi.org/10.1016/j.burns.2006.11.002.
[5] Zajicova A, et al. Treatment of ocular surface injuries by limbal and mesenchymal stem cells growing on nanofiber scaffolds. Cell Transplant 2010;19(10):1281–90. https://doi.org/10.3727/096368910X509040.
[6] Segers VFM, Lee RT. Stem-cell therapy for cardiac disease. Nature Feb. 2008;451(7181):937–42. https://doi.org/10.1038/nature06800.
[7] Roth EA, Xu T, Das M, Gregory C, Hickman JJ, Boland T. Inkjet printing for high-throughput cell patterning. Biomaterials 2004;25(17):3707–15. https://doi.org/10.1016/j.biomaterials.2003.10.052.
[8] Zhao P, Gu H, Mi H, Rao C, Fu J, sheng Turng L. Fabrication of scaffolds in tissue engineering: a review. Front Mech Eng 2018;13(1):107–19. https://doi.org/10.1007/s11465-018-0496-8.
[9] Falke G, Atala A. Reconstrucción de tejidos y órganos utilizando ingeniería tisular Actualización. Arch Argent Pediatr 2000;98.
[10] Korrapati PS, Karthikeyan K, Satish A, Krishnaswamy VR, Venugopal JR, Ramakrishna S. Recent advancements in nanotechnological strategies in selection, design and delivery of biomolecules for skin regeneration. Mater Sci Eng C Mater Biol Appl Oct. 2016;67:747–65. https://doi.org/10.1016/j.msec.2016.05.074.
[11] Thangapazham RL, Darling TN, Meyerle J. Alteration of skin properties with autologous dermal fibroblasts. Int J Mol Sci May 2014;15(5):8407–27. https://doi.org/10.3390/ijms15058407.
[12] Li A, Pouliot N, Redvers R, Kaur P. Extensive tissue-regenerative capacity of neonatal human keratinocyte stem cells and their progeny. J Clin Invest Feb. 2004;113(3):390–400. https://doi.org/10.1172/JCI19140.
[13] Fortunel NO, Vaigot P, Cadio E, Martin MT. Functional investigations of keratinocyte stem cells and progenitors at a single-cell level using multiparallel clonal microcultures. Methods Mol Biol 2010;585:13–23. https://doi.org/10.1007/978-1-60761-380-0_2.
[14] Plikus MV, Gay DL, Treffeisen E, Wang A, Supapannachart RJ, Cotsarelis G. Epithelial stem cells and implications for wound repair. Semin Cell Dev Biol 2012;23(9):946–53. https://doi.org/10.1016/j.semcdb.2012.10.001.
[15] Dabiri G, Heiner D, Falanga V. The emerging use of bone marrow-derived mesenchymal stem cells in the treatment of human chronic wounds. Expet Opin Emerg Drugs Dec. 2013;18(4):405–19. https://doi.org/10.1517/14728214.2013.833184.
[16] Jackson WM, Nesti LJ, Tuan RS. Concise review: clinical translation of wound healing therapies based on mesenchymal stem cells. Stem Cells Transl. Med. Jan. 2012;1(1):44–50. https://doi.org/10.5966/sctm.2011-0024.
[17] Arno AI, et al. Human Wharton's jelly mesenchymal stem cells promote skin wound healing through paracrine signaling. Stem Cell Res Ther 2014;5(1):1–13.
[18] Silva-Cote I, et al. Strategy for the generation of engineered bone constructs based on umbilical cord mesenchymal stromal cells expanded with human platelet lysate. Stem Cell Int 2019;2019. https://doi.org/10.1155/2019/7198215.
[19] Cheng Z, Teoh SH. Surface modification of ultra thin poly e-caprolactone) films using acrylic acid and collagen. Biomaterials 2004;25:1991–2001.
[20] Dai N-T, Williamson MR, Khammo N, Adams EF, Coombes AGA. Composite cell support membranes based on collagen and polycaprolactone for tissue engineering of skin. Biomaterials 2004;25(18):4263–71. https://doi.org/10.1016/j.biomaterials.2003.11.022.
[21] Oztemur J, Yalcin-Enis I. Development of biodegradable webs of PLA/PCL blends prepared via electrospinning: morphological, chemical, and thermal characterization. J Biomed Mater Res Part B Appl Biomater 2021;109(11):1844–56. https://doi.org/10.1002/jbm.b.34846.
[22] Tiyek I, Gunduz A, Yalcinkaya F, Chaloupek J. Influence of electrospinning parameters on the hydrophilicity of electrospun polycaprolactone nanofibres. J Nanosci Nanotechnol 2019;19(11):7251–60. https://doi.org/10.1166/jnn.2019.16605.
[23] Speranza V, Sorrentino A, De Santis F, Pantani R. Characterization of the polycaprolactone melt crystallization: complementary optical microscopy, DSC, and AFM studies. Sci World J 2014;2014:720157. https://doi.org/10.1155/2014/720157.
[24] Chen ZG, Wang PW, Wei B, Mo XM, Cui FZ. Electrospun collagen-chitosan nanofiber: a biomimetic extracellular matrix for endothelial cell and smooth muscle cell. Acta Biomater Feb. 2010;6(2):372–82. https://doi.org/10.1016/j.actbio.2009.07.024.
[25] Averous L, Moro L, Dole P, Fringant C. Properties of thermoplastic blends: starch–polycaprolactone. Polymer (Guildf) 2000;41(11):4157–67. https://doi.org/10.1016/S0032-3861(99)00636-9.
[26] Powell HM, Boyce ST. Engineered human skin fabricated using electrospun collagen-PCL blends: morphogenesis and mechanical properties. Tissue Eng Aug. 2009;15(8):2177–87. https://doi.org/10.1089/ten.tea.2008.0473.
[27] Shields KJ, Beckman MJ, Bowlin GL, Wayne JS. Mechanical properties and cellular proliferation of electrospun collagen type II. Tissue Eng 2004;10(9–10):1510–7. https://doi.org/10.1089/ten.2004.10.1510.
[28] Pérez ML, et al. Fast protocol for the processing of split-thickness skin into decellularized human dermal matrix. Tissue Cell May, 2021;72. https://doi.org/10.1016/j.tice.2021.101572.
[29] Ankersen J, Birkbeck AE, Thompson RD, Vanezis P. Puncture resistance and tensile strength of skin simulants. Proc Inst Mech Eng Part H J Eng Med 1999;213(6):493–501. https://doi.org/10.1243/0954411991535103.
[30] Zhu H, Li R, Wu X, Chen K, Che J. Controllable fabrication and characterization of hydrophilic PCL/wool keratin nanonets by electronetting. Eur Polym J 2017;86:154–61. https://doi.org/10.1016/j.eurpolymj.2016.11.023. no. November 2016.
[31] Maddaluno L, Urwyler C, Werner S. Fibroblast growth factors: key players in regeneration and tissue repair. Dev 2017;144(22):4047–60. https://doi.org/10.1242/dev.152587.
[32] Usui ML, Underwood RA, Mansbridge JN, Muffley LA, Carter WG, Olerud JE. Morphological evidence for the role of suprabasal keratinocytes in wound reepithelialization. Wound Repair Regen 2005;13(5):468–79. https://doi.org/10.1111/j.1067-1927.2005.00067.x.
[33] Ranjbarvan P, Golchin A, Azari A, Niknam Z. The bilayer skin substitute based on human adipose-derived mesenchymal stem cells and neonate keratinocytes on the 3D nanofibrous PCL-platelet gel scaffold. Polym Bull 2022;79(6):4013–30. https://doi.org/10.1007/s00289-021-03702-0.
[34] Lorden ER, et al. Biostable electrospun microfibrous scaffolds mitigate hypertrophic scar contraction in an immune-competent murine model. Acta Biomater 2016;32:100–9. https://doi.org/10.1016/j.actbio.2015.12.025.
[35] Ahn GY, Ryu T-K, Choi YR, Park JR, Lee MJ, Choi S-W. Fabrication and optimization of Nanodiamonds-composited poly (ε-caprolactone) fibrous matrices for potential regeneration of hard tissues. Biomater Res 2018;22(1):1–8.
[36] Keirouz A, Chung M, Kwon J, Fortunato G, Radacsi N. 2D and 3D electrospinning technologies for the fabrication of nanofibrous scaffolds for skin tissue engineering: a review. Wiley Interdiscip Rev Nanomed Nanobiotechnol 2020;12(4):1–32. https://doi.org/10.1002/wnan.1626.
[37] MacNeil S. Biomaterials for tissue engineering of skin. Mater Today 2008;11(5):26–35. https://doi.org/10.1016/S1369-7021(08)70087-7.
[38] Ilyas RA, et al. Natural fiber-reinforced polycaprolactone green and hybrid biocomposites for various advanced applications. Polymers (Basel) 2022;14(1):1–28. https://doi.org/10.3390/polym14010182.
[39] Christen MO, Vercesi F. Polycaprolactone: how a well-known and futuristic polymer has become an innovative collagen-stimulator in esthetics. Clin Cosmet Invest Dermatol 2020;13:31–48. https://doi.org/10.2147/CCID.S229054.
[40] Nair LS, Laurencin CT. Biodegradable polymers as biomaterials. Prog Polym Sci 2007;32(8–9):762–98. https://doi.org/10.1016/j.progpolymsci.2007.05.017.
[41] Chor A, et al. In Vitro degradation of electrospun Mucosa regeneration. Polymer (Guildf). 2020;12(1853).
[42] Hernández-Rangel A, Martin-Martinez ES. Collagen based electrospun materials for skin wounds treatment. J Biomed Mater Res, Part A 2021;109(9):1751–64. https://doi.org/10.1002/jbm.a.37154.
[43] Gautam S, Chou C-F, Dinda AK, Potdar PD, Mishra NC. Surface modification of nanofibrous polycaprolactone/gelatin composite scaffold by collagen type I

grafting for skin tissue engineering. Mater Sci Eng C Mater Biol Appl Jan. 2014;34:402–9. https://doi.org/10.1016/j.msec.2013.09.043.
[44] Ju YM, Choi JS, Atala A, Yoo JJ, Lee SJ. Bilayered scaffold for engineering cellularized blood vessels. Biomaterials May 2010;31(15):4313–21. https://doi.org/10.1016/j.biomaterials.2010.02.002.
[45] Chakrapani VY, Gnanamani A, Giridev VR, Madhusoothanan M, Sekaran G. Electrospinning of type I collagen and PCL nanofibers using acetic acid. 2012. https://doi.org/10.1002/app.
[46] Kołbuk D, Sajkiewicz P, Maniura-Weber K, Fortunato G. Structure and morphology of electrospun polycaprolactone/gelatine nanofibres. Eur Polym J 2013;49(8):2052–61. https://doi.org/10.1016/j.eurpolymj.2013.04.036.
[47] Wang Z, et al. Fabrication and in vitro evaluation of PCL/gelatin hierarchical scaffolds based on melt electrospinning writing and solution electrospinning for bone regeneration. Mater Sci Eng C 2021;128(May):112287. https://doi.org/10.1016/j.msec.2021.112287.
[48] Zhang Q, Lv S, Lu J, Jiang S, Lin L. Characterization of polycaprolactone/collagen fibrous scaffolds by electrospinning and their bioactivity. Int J Biol Macromol 2015;76:94–101. https://doi.org/10.1016/j.ijbiomac.2015.01.063.
[49] Pedersen N, et al. Low-FODMAP diet reduces irritable bowel symptoms in patients with inflammatory bowel disease. World J Gastroenterol 2017;23(18):3356–66. https://doi.org/10.3748/wjg.v23.i18.3356.
[50] Podwojewski F, Otténio M, Beillas P, Guérin G, Turquier F, Mitton D. Mechanical response of animal abdominal walls in vitro: evaluation of the influence of a hernia defect and a repair with a mesh implanted intraperitoneally. J Biomech 2013;46(3):561–6. https://doi.org/10.1016/j.jbiomech.2012.09.014.
[51] Perez-Puyana V, et al. Fabrication of hybrid scaffolds obtained from combinations of PCL with gelatin or collagen via electrospinning for skeletal muscle tissue engineering. J Biomed Mater Res, Part A 2021;109(9):1600–12. https://doi.org/10.1002/jbm.a.37156.
[52] Zhang YZ, Venugopal J, Huang ZM, Lim CT, Ramakrishna S. Characterization of the surface biocompatibility of the electrospun PCL-Collagen nanofibers using fibroblasts. Biomacromolecules 2005;6(5):2583–9. https://doi.org/10.1021/bm050314k.
[53] Han Y, et al. The secretion pro fi le of mesenchymal stem cells and potential applications in treating human diseases. 2022. https://doi.org/10.1038/s41392-022-00932-0. no. February.
[54] Garzón I, et al. Wharton's jelly stem cells: a novel cell source for oral Mucosa and skin epithelia regeneration. Stem Cells Transl Med 2013;2(8):625–32. https://doi.org/10.5966/sctm.2012-0157.
[55] Girija DM, Subbarayan R. Transdifferentiation of human gingival mesenchymal stem cells into functional keratinocytes by Acalypha indica in three - dimensional microenvironment. 2018. p. 1–8. https://doi.org/10.1002/jcp.26807. no. October 2017.
[56] Ranjbarvan P, Golchin A, Azari A, Niknam Z. Adipose - derived mesenchymal stem cells and neonate scaffold. Polym Bull 2021:0123456789. https://doi.org/10.1007/s00289-021-03702-0.
[57] Wagner N, et al. Lack of plakoglobin leads to lethal congenital epidermolysis bullosa : a novel clinico-genetic entity. Human Molecul 2011;20(9):1811–9. https://doi.org/10.1093/hmg/ddr064.
[58] Shi H, et al. The anti-scar effects of basic fibroblast growth factor on the wound repair in vitro and in vivo. PLoS One 2013;8(4). https://doi.org/10.1371/journal.pone.0059966.
[59] Liarte S. Role of TGF- β in skin chronic wounds: a keratinocyte perspective. 2020.
[60] Gilbert RWD, Vickaryous MK, Viloria-petit AM. Signalling by transforming growth factor beta isoforms in wound healing and tissue regeneration. 2016. https://doi.org/10.3390/jdb4020021.
[61] Khan M, Aziz AA, Shafi NA, Abbas T, Khanani AM. Targeting Angiopoietin in retinal vascular diseases: a literature review and summary of clinical trials. 2020. p. 1–14.
[62] McDonald DM, Gavin Thurston1 GDY, Rudge2 John S, Ioffe2 Ella, Zhou2 Hao, Ross2 Leorah, Croll2 Susan D, Glazer1 Nicole, Holash2 Jocelyn. Angiopoietin-1 protects the adult vasculature against plasma leakage. Nat Med 2000;6(4):4–7.
[63] Wang K, et al. Three-layered PCL grafts promoted vascular regeneration in a rabbit carotid artery model. Macromol Biosci 2016;16(4):608–918. https://doi.org/10.1002/mabi.201500355.
[64] Lizarazo-Fonseca L, Muñoz-Prieto E, Vera-Graziano R, Camacho B, Salguero G, Silva-Cote I. Electrospun poly (ϵ-caprolactone)/collagen scaffolds with potential use for skin regeneration. Cienc en Desarro 2019;10(2).
[65] Lorden ER, et al. Mitigation of hypertrophic scar contraction via an elastomeric biodegradable scaffold. Biomaterials 2015;43(1):61–70. https://doi.org/10.1016/j.biomaterials.2014.12.003.
[66] Choudhury S, Das A. Advances in generation of three-dimensional skin equivalents: pre-clinical studies to clinical therapies. Cytotherapy 2021;23(1):1–9. https://doi.org/10.1016/j.jcyt.2020.10.001.
[67] Jones I, Currie L, Martin R. A guide to biological skin substitutes the function of normal skin. Br J Plast Surg Br Assoc Plast Surg 2002;55:185–93. https://doi.org/10.1054/hips.2002.3800.
[68] Alrubay L, Al-Rubay KK. Skin substitutes: a brief review of types and clinical applications. 2009.
[69] Cruz-Barrera M, et al. Integrated analysis of transcriptome and secretome from umbilical cord mesenchymal stromal cells reveal new mechanisms for the modulation of inflammation and immune activation. Front Immunol 2020;11:1–19. https://doi.org/10.3389/fimmu.2020.575488. no. September.